COMSOL
CONFERENCE
2023 MUNICH

Computational Modeling of a Plasma Torch Using Single-Fluid and Two-Fluid Modeling Approaches

S.L. Siddanathi[1], L.G. Westerberg[1], H.O. Åkerstedt[1], H. Wiinikka[2], A. Sepman[2]
1. Division of Fluid- and Experimental Mechanics, Luleå University of Technology, SE-971 87 Luleå, Sweden
2. RISE AB, SE-941 38 Piteå, Sweden.

Abstract
Plasma, a complex fluid consisting of electrons, ions, neutrals, and excited species, exhibits both fluid-like behavior and electrical conductivity due to the presence of charge carriers. Consequently, computational modeling of plasma requires the integration of fluid and electrical models. This research paper presents a study on the steady-state computational modeling of a plasma torch with a 2D axisymmetric geometry using single-fluid and two-fluid modeling approaches in the COMSOL Multiphysics® software. The single-fluid modeling (SFM) approach combines the individual equations governing the behavior of different particles into a unified equation. Specifically, the SFM approach utilized in this study focuses on a fully ionized plasma and employs the Magnetohydrodynamic equations whose adaptation is equilibrium discharge interface (EDI) model available in COMSOL Multiphysics®. The EDI model solves the magnetohydrodynamic (MHD) equations, encompassing electric and magnetic fields, heat transfer in solids and fluids, and laminar models. By employing this approach, the researchers simulated and analyzed the behavior of the plasma torch. In contrast, the two-fluid modeling (TFM) approach separates the fluid equations for electrons and ions, considering a weakly ionized plasma. The TFM model is developed by deriving fluid equations based on kinetic theory for neutrals, ions, and electrons. These equations are then implemented in COMSOL Multiphysics®, utilizing models for the transport of diluted species, laminar flow, heat transfer in solids and fluids, and electric and magnetic fields. By adopting the TFM approach, the researchers aimed to gain insights into the behavior of the plasma torch. Throughout the study, various properties such as temperature, velocity, current density, and particle concentrations are analyzed within the plasma torch. Results obtained from both the single-fluid and two-fluid modeling approaches are compared and evaluated. This comparative analysis allows the researchers to highlight the advantages and challenges associated with each modeling approach. In conclusion, this study contributes to understanding plasma behavior by employing computational modeling techniques. The research presents and compares the outcomes of single-fluid and two-fluid modeling approaches applied to a plasma torch. By examining the advantages and challenges of each approach, the study offers valuable insights for future plasma modeling endeavors.

Keywords: non-transferred plasma torch, Magnetohydrodynamics, weak ionization.

Introduction
A DC non-transferred plasma torch is a source to generate steady thermal plasma. It consists of a thoriated tungsten cathode tip, a copper anode, and a working gas. Power is initiated at the cathode tip, resulting in a voltage differential, and establishing an electric arc between the electrodes. The working gas, introduced close to the cathode, is channeled through. As this gas encounters the arc, the arc extends and increases the voltage. Plasma formation occurs due to Joule heating from the arc current, which ionizes and warms the gas. This shift to a plasma state leads to a swift rise in the gas/plasma's velocity and temperature. Moreover, the arc current's interaction with its self-generated magnetic field creates a Lorentz force, propelling the plasma jet to the exit [1].

From the working principle of the non-transferred plasma torch, it could be understood that the combination of fluid dynamics, heat flow and electromagnetic effects are required to describe flow in a non-transferred plasma torch. The computational modeling of flow inside a non-transferred plasma torch can be done by solving magnetohydrodynamic (MHD) equations in the form of single fluid equations (SFE) or two fluid equations (TFE). The SFE are obtained by combining the electron and ions equations together to obtain equations governing the plasma described as single fluid. Whereas the TFE are the ones that apply to electrons and ions separately and both the fluids are tracked separately. Modeling the plasma using SFE where the temperature of electrons and ions are assumed to be equal is simple and widely used approach. The details such as velocity, temperature and current distribution of the plasma jet can be accurately predicted by solving SFE [1, 2, 3]. The fully ionized plasma and charge neutral plasma is assumed to be valid everywhere in the plasma torch. But the flow properties near the sheath region and the rate of ionization is hard to predict using SFE and TFE are required to understand the flow in the plasma torch in detail [4].

Therefore, this paper explains theory of magnetohydrodynamic equations, single fluid equations and two fluid equations. Followed by adaptation of the equations to model in COMSOL Multiphysics v6.1. The results presented explains the details of the velocity, temperature, rate of ionization

and current distribution. The paper is concluded by stating the advantages and disadvantages of computational modeling using SFE and TFE.

Plasma Models Theory and Equations

One of easiest ways to computationally model the flow in plasma torch is by using MHD equations. In MHD, the discharge current generates a magnetic field and the plasma flow together with the magnetic field further increases the current and magnetic fields. A self-consistent set of ideal MHD equations co-relate the plasma mass density, velocity, thermodynamic pressure, electric field and magnetic field.

In this paper, the two computational models that can be used to analyze flow in non-transferred plasma torch are presented. Their equations and assumptions are explained below.

Weakly Ionized Plasma (WIP) Model

Based on the particle interactions a plasma can be classified as either weakly ionized or strongly ionized. The WIP model is perhaps next to MHD the simplest plasma model. But it can be developed further to describe partially ionized plasma in which number density of electrons and ions is approximately equal to n. In WIP, the charge neutral interactions dominate over multiple coulomb interactions. A WIP is a multi-component plasma that is a combination of electrons, ions, and neutrals respectively, and in which the number density of ions and electrons is very much less than the number density of neutrals, i.e. $n_i, n_e \ll n$. The WIP model is derived from kinetic theory of a simple gas, in which the collision frequency is considered according to $\nu_{nn} \gg \nu_{ni}, \nu_{ne} \gg \nu_{ii}, \nu_{ie}, \nu$. The assumptions made to derive WIP model are:

1. $\nu_{en} \gg \nu_{in} \gg \nu_{ei}$
2. Inertia terms are neglected
3. In the main part of the plasma, $n_i = n_e$. But the condition is not applied near the walls.

In table 1 a summary of WIP model equations are presented, while in this section complete details of theIP equations and boundary conditions are presented.

The steady state equations of motion for electrons, ions and neutrals reads [5]

$$\textbf{Neutrals}: nm\left\{\frac{\partial \boldsymbol{u}}{\partial t} + (\boldsymbol{u}.\nabla)\boldsymbol{u}\right\} = -\nabla p + \nabla.\left\{\mu(\nabla \boldsymbol{u}) + (\nabla \boldsymbol{u})^T - \frac{2}{3}\mu \nabla.\boldsymbol{u}\right\} - nn_i m_{in}\nu_{in}(\boldsymbol{u} - \boldsymbol{u_i}) - nn_e m_{en}\nu_{en}(\boldsymbol{u} - \boldsymbol{u_e}) \quad [1]$$

$$\textbf{Ions}: n_i m_i\left\{\frac{\partial \boldsymbol{u_i}}{\partial t} + (\boldsymbol{u_i}.\nabla)\boldsymbol{u_i}\right\} = -\nabla p_i - n_i n m_{in}\nu_{in}(\boldsymbol{u_i} - \boldsymbol{u}) - n_i \boldsymbol{u_e} m_{ie}\nu_{ie}(\boldsymbol{u_i} - \boldsymbol{u_e}) + n_i e(\boldsymbol{E} + \boldsymbol{u_i} \times \boldsymbol{B}) \quad [2]$$

$$\textbf{Electrons}: n_e m_e\left\{\frac{\partial \boldsymbol{u_e}}{\partial t} + (\boldsymbol{u_e}.\nabla)\boldsymbol{u_e}\right\} = -\nabla p_e - n_e n m_{en}\nu_{en}(\boldsymbol{u_e} - \boldsymbol{u}) - n_e \boldsymbol{u_i} m_{ie}\nu_{ei}(\boldsymbol{u_e} - \boldsymbol{u_i}) - n_e e(\boldsymbol{E} + \boldsymbol{u_e} \times \boldsymbol{B}), \quad [3]$$

where the reduced mass is $m_{\alpha\beta} = \frac{m_\alpha m_\beta}{m_\alpha + m_\beta}$ [4]

and

$$\nu_{in} = \sigma_{in}\sqrt{\frac{8kT}{\pi m_{in}}}, \sigma_{in} = 2\pi(r_i + r_n)^2$$
$$\nu_{en} = \sigma_{en}\sqrt{\frac{8kT}{\pi m_{en}}}, \sigma_{en} = 2\pi(r_e + r_n)^2. \quad [5]$$

The single fluid equation is obtained by introducing center of mass velocity,

$$\boldsymbol{U} = \frac{n_e m_e \boldsymbol{u_e} + n_i m_i \boldsymbol{u_i} + nm\boldsymbol{u}}{n_e m_e + n_i m_i + nm}. \quad [6]$$

Adding equations 1-3, that are equations of motion for all the species and adding all energy equations for all species and introducing current density,

current density, $\boldsymbol{j} = n_i e \boldsymbol{u_i} - n_e e \boldsymbol{u_e}$. [7]

The equation of motion reads

$$\rho \frac{D\boldsymbol{U}}{Dt} = -\nabla.\pi + \boldsymbol{j} \times \boldsymbol{B}, \quad [8]$$

Energy equation

$$\rho c_p \frac{DT}{Dt} + \nabla.\boldsymbol{q} = \boldsymbol{j}.\boldsymbol{E} = \frac{j^2}{\sigma} \quad [9]$$

$$\boldsymbol{q} = -\frac{5}{2}\frac{n\boldsymbol{k}T}{m\nu_{nn}}\nabla(uT) + \frac{5}{2}\frac{n_e \boldsymbol{u}T}{m_e \nu_{en}} e\boldsymbol{E}. \quad [10]$$

In the right-hand side of equation 10, the first term comes from neutrals, ordinary heat conduction and the second term is an extra term, heat conductivity due to σ.

Further, solving for velocity in equation 2 and 3 diffusion equations are obtained as follows,

$$\boldsymbol{u_i} = \boldsymbol{u} - \frac{1}{n_i}\nabla\left(\frac{kT_i}{m_i \nu_{in}} n_i\right) + \frac{e}{m_i \nu_{in}}\boldsymbol{E}$$
$$\boldsymbol{u_e} = \boldsymbol{u} - \frac{1}{n_e}\nabla\left(\frac{uT_e}{m_e \nu_{en}} n_e\right) + \mu_e \boldsymbol{E} \quad [11]$$
$$D_i = \frac{kT_i}{m_i \nu_{in}}, \mu_i = \frac{e}{m_i \nu_{in}}$$
$$D_e = \frac{kT_e}{m_e \nu_{en}}, \mu_e = \frac{e}{m_e \nu_{en}}. \quad [12]$$

Together with the equation for conservation of particles, ionization, and recombination this gives:

$$\nabla.(n_e \boldsymbol{u}) - \nabla.\{D_{en}\nabla n_e\} + \nabla.(\mu_e.\boldsymbol{E}) = k_i n n_e - k_{\lceil} n_e^3 \quad [13]$$
$$\nabla.(n_i \boldsymbol{u}) - \nabla.\{D_i \nabla n_i\} + \nabla.(\mu_i.\boldsymbol{E}) = k_i n n_e - k_{\lceil} n_e^3 \quad [14]$$

From the literature the following equations describing ionization and recombination are obtained:

$$n_{eq} = \left(n_o 2.041.10^{21} T^{\frac{3}{2}} e^{\frac{-1.68.10^5}{T}}\right)^{\frac{1}{2}} m^{-3},$$

$$G = 2.045.10^{21} T^{\frac{3}{2}} e^{\frac{-1.68.10^5}{T}},$$

$$\alpha = 1.29.10^{-44}\left(2 + \frac{1.353.10^5}{T}\right) e^{\frac{4.78.10^4}{T}} m^6/s$$ [6, 7, 8]. [15]

Further, derivation of charge neutrality is as follows, where equation 16a and 16b describes the particle flux and equations 17a and 17b describes mobility.

$$\boldsymbol{J_i} = n_i \boldsymbol{u_i} = n_i \boldsymbol{u} - \frac{kT_i}{m_i v_{in}} \nabla n_i + n_i \mu_i \boldsymbol{E}$$ [16a]

$$\boldsymbol{J_e} = n_e \boldsymbol{u_e} = n_e \boldsymbol{u} - \frac{kT_e}{m_e v_{en}} \nabla n_e - n_e \mu_e \boldsymbol{E}\,.$$ [16b]

$$\mu_e = \frac{e}{m_e v_{en}}$$ [17a]

$$\mu_i = \frac{e}{m_i v_{in}}.$$ [17b]

Conservation of charge and charge neutrality are as follows:

$$\nabla . \boldsymbol{j} = 0$$ [18]

$$\nabla . \left((n_i - n_e) e \boldsymbol{u}\right) - \nabla . (e D_i \nabla n_i - e D_e \nabla n_e) + \nabla . \left((n_i \mu_i e + u_e \mu_e e) \boldsymbol{E}\right) = 0$$ [19]

From the third assumption the following term is equalized to zero,

$$-\nabla . \{e(D_i - D_e)\nabla n\} + \nabla . (n(\mu_i + \mu_e) e \boldsymbol{E}) = 0$$ [20]

Further, solving for electric field the solution can be divided into a partial solution and a homogeneous solution,

$$\boldsymbol{E} = \boldsymbol{E_p} + \boldsymbol{E_H}$$ [21]

$$\nabla . \left(\left(\frac{ne^2}{v_{in} m_i} + \frac{ne^2}{v_{en} m_e}\right) \boldsymbol{E_H}\right) = 0 \text{ (conductivity)},$$

$$\nabla . (\sigma . \boldsymbol{E_H}) = 0 \text{ (Ohm's law)}.$$ [22]

Solution Ep is chosen as follows,

$$\boldsymbol{E_p} = \frac{D_i - D_e}{\mu_i + \mu_e} \frac{\nabla n}{n}.$$ [23]

Therefore, following the third assumption, diffusion equations 13 and 14 becomes as follows,

$$\nabla . (n_e \boldsymbol{u}) - \nabla . (D_a \nabla n_e) = k_i n_e n - k_{\text{l}} n_e^3$$ [24a]

$$\nabla . (n_i \boldsymbol{u}) - \nabla . (D_a \nabla n_i) = k_i n_e n - k_{\text{l}} n_e^3.$$ [24b]

These are convective diffusion equations with ambipolar diffusion and no electric field. Since $n_i = n_e$ only one equation is needed. Thus, the Ambipolar diffusion term by eliminating one part of electric field,

$$D_a = \frac{\mu_i D_e - \mu_e D_i}{\mu_i + \mu_e}.$$ [25]

Boundary conditions for electron density

The cathode in the plasma torch is an emitting cathode that has thermionic effect and work function. Therefore, the boundary condition at cathode is obtained from literature [9].

$$n_e = \frac{4 \boldsymbol{J_R}}{e v_{th}}.$$ [26]

The usual boundary condition at the anode is $n_e = 0$. This leads to a problem as $\sigma \to 0$ at the wall [10].

The charge neutrality is however not valid in the region close to the wall. Here, there is a thin plasma sheet in which number density of electron is not equal to number density of ions. To circumvent this problem without including the plasma sheet in the numerical model we use the outer edge solution of the plasma sheet model by Benilov at anode [9],

$$\frac{\partial n_e}{\partial n} = 0$$ [27]

Magnetohydrodynamics (EDI) model

The MHD (EDI) model is used to model a fully ionized flow in a non-transferred plasma torch. A plasma is said to be fully ionized when the degree of ionization is such that the multiple coulomb interaction become dominant. The fully ionized plasma is combination of electrons and ions alone. The EDI model in COMSOL is an adaptation of single fluid MHD equations. The details of the material properties and solver conditions that are good for EDI modeling are explained in our previous works but in table 2 a summary of equations in the EDI model are presented.

Table 1: *Summary of WIP model equations*

Model	Equations
Laminar flow	$\rho \frac{\mathrm{DU}}{\mathrm{Dt}} = -\nabla . \mathrm{p} + \mathbf{j} \times \mathbf{B}$
Transport of diluted species	$\nabla . (\mathrm{n_e}\mathbf{u}) - \nabla . (\mathrm{D_a} \nabla \mathrm{n_e}) = \mathrm{k_i n n_e} - \mathrm{k_{\text{l}}} \mathbf{u}_\mathrm{e}^3$
Electric currents	$\nabla . \left(\left(\frac{\mathrm{n_e e^2}}{\mathrm{m_e} v_{en}} + \frac{\mathrm{n_i e^2}}{\mathrm{m_i} v_{in}}\right) \mathbf{E}\right) = 0$
Heat transfer in fluids and solids	$\rho \mathrm{c_p} \frac{\mathrm{DT}}{\mathrm{Dt}} = \nabla . (\mathrm{k} \nabla \mathrm{T}) + \frac{\mathrm{j}^2}{\delta} - \frac{5}{2} \frac{\mathrm{v}}{\mathrm{e}} \mathbf{j} . \nabla \mathrm{T}$

Table 2: *Summary of EDI model equations*

Model	Equations
Laminar flow	$\frac{\partial \rho}{\partial \mathrm{t}} + \nabla . (\rho \mathbf{u}) = 0$ $\rho \left(\frac{\partial \mathbf{u}}{\partial \mathrm{t}} + \mathrm{u} . \nabla \mathbf{u}\right) = -\nabla \mathrm{p} - \nabla \tau + \mathbf{j} \times \mathbf{B}$
Heat transfer in fluids and solids	$\rho \mathrm{c_p} \left(\frac{\partial \mathrm{T}}{\partial \mathrm{t}} + \mathrm{u} . \nabla \mathrm{T}\right) = \nabla . (\mathbf{k} \nabla \mathrm{T}) + \mathbf{j} . \mathbf{E} - 4\pi \varepsilon_\mathrm{r} + \frac{5}{2} \frac{\mathrm{k_B}}{\mathrm{e}} \mathbf{j} . \nabla \mathrm{T} - \left(\frac{\partial \ln \rho}{\partial \ln \mathrm{T}}\right) \frac{\mathrm{Dp}}{\mathrm{Dt}}$
Electric current	$\nabla . \mathbf{J} = \mathrm{Q(j, v)}$ $\mathbf{J} = \sigma \mathbf{E} + \sigma \mathbf{u} \times \mathbf{B} + \mathbf{J_{eo}}, \mathbf{E} = -\nabla \mathrm{V}$
Magnetic field	$\nabla \times \mathbf{H} = \mathbf{J}$ $\mathbf{B} = \nabla \times \mathbf{A}$

Computational Setup

In the present study, the computational analysis was carried out using COMSOL Multiphysics V.6 and V6.1 to analyze a two-dimensional (2D)

axisymmetric geometry, illustrated in Figure 1. The cathode and anode materials are designated as tungsten and copper, respectively, with nitrogen functioning as the working gas. For the MHD (EDI) model, thermodynamic properties of the nitrogen, such as density, thermal conductivity, specific heat, and viscosity are defined based on conditions for fully ionized nitrogen. These specifications have been elaborated upon in our preceding publication [11]. In contrast, for the weakly ionized model, nitrogen's thermodynamic properties are calculated from the formulation to predict transport properties of gases at low densities in transport phenomena [12]. The chosen discretization method for the geometry employs an unstructured triangular mesh, comprising 17,695 elements. A steady-state analysis was executed via a fully coupled approach using the PARDISO solver. Detailed boundary conditions for the EDI and weakly ionized plasma models can be referenced in Tables 1 and 2. Further, the simulations are run for different tuning parameters that are used in transport of diluted species model for inconsistent stabilization. The parameter is used to add extra artificial diffusion and the parametric study is done within the range of 0-1000. However, the results presented in the present paper is for the case of tuning parameter 0.

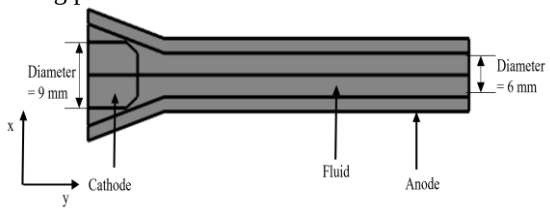

Figure 1. Schematic of 2D axisymmetric geometry used in for computational analysis.

Table 3: *Boundary conditions for MHD (EDI) model for fully ionized plasma case*

Model	Applied regions	Boundary conditions
Electric current	Fluid, cathode and anode	Normal surface current = 2e5 (cathode tip) Ground = anode
Magnetic field	Fluid and anode	$\psi_0 = 1\mathrm{A/m}$ Magnetic insulation
Heat transfer	Fluid, anode and cathode	T=3500 K (cathode tip), T_{ustr}=300 K, h=10^4W/m^2.K (anode), T_{ext}= 500 K
Laminar flow	Fluid	$u_{phi} = u_z = 5.53\,\frac{\mathrm{m}}{\mathrm{s}}$

Results

In this section, the flow changes such as velocity, temperature and current distribution inside the plasma torch are presented. Further, a comparison is made by the results obtained by using MHD (EDI) and weakly ionized plasma models for same input conditions.

Table 4*: Boundary conditions for Weakly ionized plasma model*

Model	Applied regions	Boundary conditions
Transport of diluted species	Fluid	$c_{initial}$=1e-8 mol/m^3, c_{inlet}=1e-9 mol/m^3, $c_{cathode\ tip}$=5.5e-4 mol/m^3
Electric current	Anode and fluid	J_n=4.5e5 A/m^2 (cathode tip), ground = anode
Magnetic field	Anode and fluid	$\psi_0 = 1\mathrm{A/m}$ Magnetic insulation
Heat transfer	Anode, cathode and fluid	T=3500 K (cathode tip) h=10^4 W/m^{2}K, T_{ext} = 400 K (anode)
Laminar flow	fluid	$u_{phi} = u_z = 5.53\ m/s$

Velocity variations

Literature reviews highlight a significant acceleration in velocity at the cathode tip. This acceleration is primarily ascribed to the gaseous expansion that arises from the interaction of the working gas with the current introduced at the cathode tip, as referenced in [1]. Figure 2 provides a comparative analysis of velocity trends as interpreted by both the WIP and MHD (EDI) models. In this comparison, data is mapped from the cathode tip to the outlet, reflecting an input power setting of 0.1 kW and a velocity parameter of 11.06 m/s. As inferred from Figure 2, the WIP model prognosticates a rise in velocity at the cathode tip. In contrast, the MHD (EDI) model delineates a minor flow separation at this very tip, which subsequently gives way to an increase in velocity as we move towards the outlet.

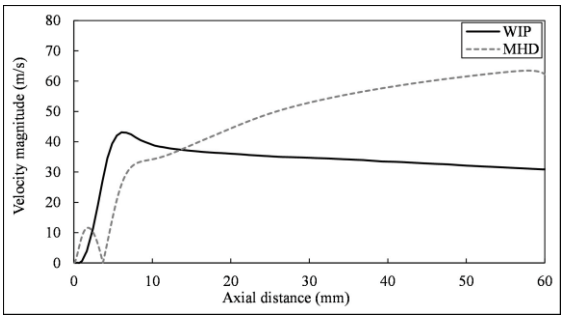

Figure 2. Comparison of velocity variation of plasma jet inside the plasma torch using WIP and MHD (EDI) models at 0.1 kW input power.

The flat contour of the cathode tip, in fluid dynamic parlance, can be interpreted as instigating flow separation due to its abrupt geometric transition. Furthermore, in scenarios where electromagnetic forces couple with plasma genesis at the cathode tip, such flow separations can be negated. Regrettably, the MHD (EDI) model seems to fail in mitigating this separation at the cathode tip at this low input power, rendering a velocity profile that diverges from the archetypal profile witnessed in a non-transferred plasma torch. Conversely, the WIP

model intimates a steady decrease in velocity as one approaches the outlet—a trajectory that resonates with the quintessential dynamics of plasma jets, as endorsed by preceding studies [1, 3, 6].

Temperature variations

Figure 3 explains the temperature variations as discerned from the WIP and MHD (EDI) models. The data trajectory spans from the cathode tip to the outlet, given an input power of 0.1 kW and an inlet velocity of 11.6 m/s. Like velocity, the temperature also increases at the cathode tip, a phenomenon attributed to ionization. Both WIP and MHD (EDI) models consistently predict this temperature escalation at the cathode tip and a subsequent decline towards the outlet, resulting from anode-induced cooling. Nevertheless, there exists a noticeable disparity in the temperature approximations between the two models at the cathode tip. Specifically, the WIP model estimates the ionization temperature to be 37% elevated compared to the MHD (EDI) model. It's pertinent to note that in the MHD (EDI) model, thermodynamic properties are established for a state of fully ionized plasma gas. Drawing upon insights from the Thermal Plasma literature, it's highlighted that the onset of ionization for a gas typically transpires around 18,000 K [13]. Contrastingly, the maximum temperature forecasted by the MHF (EDI) model at the cathode tip is 5200 K. Given this discrepancy, discerning whether effective plasma formation occurs at such a temperature necessitates the computation of the ionization rate. However, by using the MHD (EDI) model the amount of ionization cannot be calculated as the plasma is assumed to be one single fluid that is in local thermal equilibrium [13].

Ionization and Concentration

Quantifying the degree of ionization is imperative, as it offers insights into the dynamics of plasma formation and elucidates the characteristics of the resultant plasma. The WIP model provides a mechanism to estimate the ionization rate. As depicted in Figure 4, the ionization rate—spanning from the cathode tip to the outlet—is showcased for varying input current magnitudes, all maintaining a consistent velocity of 11.06 m/s. A noticeable trend from the graph is the positive correlation between ionization rate and input current: as the latter escalates, so does the former. Concurrently, as the ionization rate augments, there's a corresponding rise in both temperature and velocity.

In Figure 5, the concentration of ionized nitrogen atoms and electrons. A salient observation from this illustration is the pronounced concentration peak at the cathode tip—the very locus where the working gas engages with the current, culminating in ionization and subsequent plasma generation. The concentration is peak at the cathode tip is also because the plasma is charge neutral everywhere except very close to cathode and anode where there is plasma sheet. Moreover, a direct relationship is evident between the electron concentration and the magnitude of input current, the concentration surges with intensifying current.

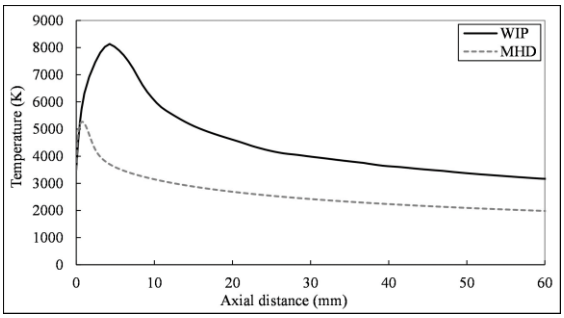

Figure 3. Comparison of Temperature variation of plasma jet inside the plasma torch using WIP and EDI models at 0.1 kW input power.

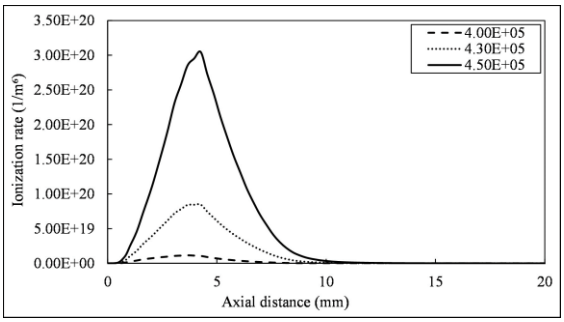

Figure 4. Ionization rate for different input currents using WIP model.

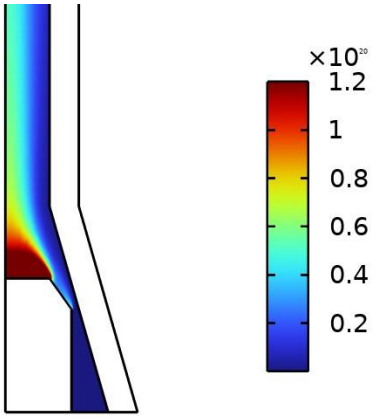

Figure 5. Concentration of electrons captured using WIP model.

Current distribution

Figure 6 presents the current density distribution across the inner walls of the anode. This graphical representation assists in pinpointing the precise location where the arc emanating from the cathode tip affixes itself to the anode. A visible peak in the current density distribution is evident approximately at 10 mm in Figure 6. This specific locus is indicative of the arc's attachment point to the anode. Contrasting this with other observations, it's noteworthy that both the WIP and MHD (EDI) models converge in their prediction of the arc attachment point. However, a subtle discrepancy emerges in the magnitude of current density: the MHD (EDI) model yields very low current density relative to the WIP model. One of the reasons behind the very low current in the arc is due to the separation. As explained previously, the arc forms at the

cathode tip and when the flow separation occurs at the very point, it disturbs the arc and reduces the current in the arc.

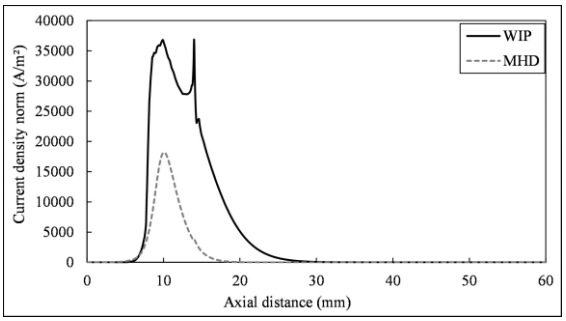

Figure 6. Comparison of current density variation of plasma jet inside the plasma torch using WIP and EDI models at 0.1 kW input power.

Conclusions

Computational modelling of plasma presents inherent complexities, chiefly owing to its multifluid characteristics. Additionally, effective computational simulations necessitate an amalgamation of electromagnetic models with fluid dynamic counterparts. To address this, this paper introduces two distinct computational models suitable for elucidating the physics underlying a DC non-transferred plasma torch: the Weakly Ionized Plasma (WIP) model and the MHD (Equilibrium Discharge Interface (EDI)) model.

The MHD (EDI) model is an integrated feature within the COMSOL Multiphysics software suite. For the sake of initiating our exploration on straightforward grounds, we commenced with the MHD (EDI) model. Subsequently, we ventured into the development of the WIP model. Analysing the computational outcomes of both these models furnishes us with a spectrum of their inherent traits, merits, and limitations:

1. Foremost, the MHD (EDI) modeling approach operates on the assumption that the plasma is fully ionized and behaves as a singular fluid. This predicates that only one cohesive set of equations is simulated. In contrast, the WIP model modulates the ionization degree based on the input current, and the interplay between electrons and ions is modelled in a distinct fashion.
2. The WIP model offers precise predictions concerning the ionization rate and the overarching trends of plasma properties. However, convergence in the solutions is predominantly observed for more modest power levels (capped at 0.1 kW). The reasons for the low convergence is because the model dilute species requires the concentration of electrons to be small, but the value is much larger where the electron concentration is $10^{20}/m^{3,}$ but the gas concentration is $10^{23}/m^3$. Further, considering a comparison of the temperature gradients at the cathode of WIP and MHD models with sharper gradient in the WIP model, can be another reason for convergence problems. This poses challenges for validation, given that a majority of empirical investigations delve into higher power ranges.
3. The results obtained by the MHD (EDI) model at low power fail to match the plasma jet profiles, because the complete ionization of nitrogen gas happens at 18000 K for nitrogen, and at low powers due to flow separation and low temperature at cathode tip the complete ionization could not happen. However, the MHD (EDI) model facilitates converged solutions at elevated power levels. Moreover, outcomes derived from the MHD (EDI) model at these higher tiers align congruently with experimental findings, as delineated in our preceding publications [6].

Upon scrutinizing the results gleaned from both the MHD (EDI) and WIP models, one can infer that each offers valuable insights into the physics of non-transferred plasma torches, albeit with distinct advantages and drawbacks. Looking ahead, our aspiration is to refine the WIP model, to be valid for a partially ionized plasma with no restriction of the degree of ionization and enabling its operation at more substantial power levels, thereby enhancing our understanding, and ensuring a more robust validation of the models. Further, the case studies regarding the flow separation at the cathode tip were conducted and will be presented in the future papers.

References

[1] R.Westhoff, and J.Szekely. "A model of fluid heat flow, and electromagnetic phenomena in a nontransferred arc plasma torch," *Journal of applied physics* , pp. 3455-3466, 70.7(1991).

[2] R.Huang, H.Fukanuma, Y.Uesugi, and Y.Tanaka. "Simulation of arc root fluctuation in a DC non-transferred plasma torch with three dimensional modeling," *Journal of thermal spray technology*, pp. 21, pp.636-643., 2012.

[3] B. Chiné, "A 2D model of a DC plasma torch," in *Comsol Conference (Vol. 2016, pp. 12-14)*., 2016, October.

[4] R. Huang, H.Fukanuma, Y.Uesugi, and Y.Tanaka. "Comparisons of two models for the simulation of a DC arc plasma torch," *Journal of thermal spray technology*, vol. 22, pp. 183-191, 2013.

[5] S.I.Braginskii, Reviews of plasma physics, Consultants Bureau New York, 1965.

[6] J. A. Bittencourt, Fundamentals of plasma physics, Springer Science & Business Media, 2004.

[7] M. E. Franke, Effects of electrostatic fields on free-convection heat transfer from plates in air, The Ohio State University, 1967.

[8] L.Sansonnens, J.Haidar, and J.J.Lowke. "Prediction of properties of free burning arcs including effects of ambipolar diffusion," *Journal of Physics D: Applied Physics*, vol. 33, no. 2, p. 148, 2000.

[9] M.S.Benilov. "Theory of a collision-dominated space-charge sheath on an emitting cathode," *Journal of Physics D: Applied Physics*, vol. 30, no. 7, p. 1115, 1997.

[10] L.Sansonnens, J.Haidar, and J.J.Lowke. "Prediction of properties of free burning arcs including effects of ambipolar diffusion," *Journal of Physics D: Applied Physics*, vol. 33, no. 2, p. 148, 2000.

[11] S.L. Siddanathi, L.G. Westerberg, H.O. Åkestedt, H. Wiinikka, A. Sepman. "Computational modeling and temperature measurements using emission spectroscopy on a non-transferred plasma torch," *AIP Advances*, vol. 13, no. 2, 2023.

[12] W.J.Beek, K.M.K.Muttzall, andVan Heuven Transport phenomena, Wiley Chichester, 1999.

[13] M.I.Boulos, P.L.Fauchais, E.Pfender. Handbook of Thermal Plasmas, Springer, 2019.

Acknowledgements
The work was funded by Swedish Energy Agency, project no. 49609-1.